DS_n-method with artificial dissipation and DMT-method of iteration acceleration for the numerical solution of 2D heat transfer equations in kinetic approximation

A.D. Gadzhiev, V.N. Seleznyov, A.A. Shestakov

This report discusses the DDAD technique used to solve the problem of radiation transport, accounting for the radiation spectrum, in 2D axi-symmetric geometry. The technique is based on the DS_n - method of solving the kinetic equation.

The DDAD technique solves the transport equation within the framework of the linear two-point scheme. The idea of this technique is in the introduction of the specially selected artificial dissipation depending on the optical thickness. Thus constructed scheme was called DDAD-(Diamond Difference with the Artificial Dissipation) scheme.

Acceleration of the iteration convergence is a very important factor in improving efficiency of simulations solving the equations of radiation transport. To accelerate the iteration convergence, the diagonal matrix technique (DMT) is implemented in the DDAD technique. If, similarly to Jacoby iterations, radiation density at some point in the system of radiation transport equations is expressed via the Planck function at the same point, and then substituted in the energy equation, the obtained system of the equations will give a diagonal matrix with respect to temperature. Using the obtained temperature, it is possible to solve the initial system either by running 1D case or with iteration methods in 2D case.

Section 1 of the report describes the DDAD numerical technique. Section 2 analyzes the results of simulation of the test problems.

1. Numerical technique DDAD

Considers a 2D non-stationary equation of radiation transport with axial symmetry in multi-group approximation:

$$\frac{1}{c}\frac{dJ_g}{dt}+div\left(\vec{\Omega}J_g\right)+\alpha_g J_g=\frac{\alpha_{sg}}{4\pi}\int_{\vec{\Omega}}J_g d\vec{\Omega}+\frac{\alpha_{cg}}{4\pi}B_g(T),\ \ g=1,2,...,G, \qquad (1.1)$$

where t is time, c is velocity of light, ρ is material density, T is material temperature,

$\vec{\Omega}$ is a unity vector in the direction of photon path,
g is group index, $g=1,2,...,G$, ε_g is energy of photons in g group,

$J_g(t,r,z,\mu,\phi)=\int_{\Delta\varepsilon_g}J(t,r,z,\mu,\phi,\varepsilon)d\varepsilon$ is radiation intensity of g-group photons flying in

$\vec{\Omega}$ direction,

$\alpha_g(t,\vec{r})$ is an attenuation coefficient of the g-group photons,

$\alpha_{cg}(t,\vec{r})$ is an absorption coefficient of the g-group photons,

$\alpha_{sg}(t,\vec{r})$ is coefficient of scattering of photons from the g-group,

$B_g=\frac{8\pi}{c^2h^3}\int_{\Delta\varepsilon_g}\frac{\varepsilon^3}{\exp\frac{\varepsilon}{T}-1}d\varepsilon$ is the Planck function for the g-group, h is the Planck constant.

The following energy equation is solved jointly with the equations of radiation transport (1.1):

$$\rho\frac{\partial E}{\partial t}=\sum_{g=1}^{G}\alpha_{cg}\int_{\vec{\Omega}}(J_g-\frac{1}{4\pi}B_g)d\vec{\Omega}+\rho Q, \qquad (1.2)$$

where Q is an external source.

Numerical algorithm exploits the transport equation written in cylindrical coordinates (r,z). For the kinetic equations, coordinate form of operator $div(\vec{\Omega}J)$ is as follows:

$$div\left(\vec{\Omega}J\right)=\frac{1}{r}\frac{\partial}{\partial r}\left(r\xi J\right)+\frac{\partial}{\partial z}\left(\mu J\right)-\frac{1}{r}\frac{\partial}{\partial\phi}\left(\eta J\right), \qquad (1.3)$$

where $\mu=\cos\theta,\xi=\sqrt{1-\mu^2}\cos\phi,\eta=\sqrt{1-\mu^2}\sin\phi,$

θ is an angle between $\vec{\Omega}$ and axis $\vec{z}$, ϕ is an angle between $\vec{r}$ and projection of $\vec{\Omega}$ onto the plane perpendicular to the $\vec{z}$ axis.

An arbitrary quadrilateral mesh with nodes $(r,z)_{ij}$ is used for space coordinates, and ES_n-quadrature [2] is used for the angles μ and ϕ .

Integrating equation (1.1) over the mesh cell, obtain:

$$\frac{1}{c\Delta t^n}\left[\left(J_g\right)^{n+1}-\left(J_g\right)^n\right]+div_h(\vec{\Omega}J_g^{n+1})+\alpha_g J_g^{n+1}=Q_g^{n+1}, \qquad (1.4)$$

$$Q_g^{n+1}=\frac{1}{4\pi}\left(\alpha_{sg}U_g^{n+1}+\alpha_{cg}B_g^{n+1}\right),$$

$$U_g = \sum_{m=1}^{M}\sum_{k=1}^{K_m} J_g \Delta\mu_{m-1}\Delta\phi_{k-1},\ g = 1,2,...,G_1.$$

Fractional indices are omitted as usual. For example, $J_g^{n+1} = (J_g)^{n+1}_{i+\frac{1}{2},j+\frac{1}{2},k-\frac{1}{2},m-\frac{1}{2}}$.

Difference operator $div_h(\cdot)$ has the following meaning:

$$div_h(\vec{\Omega}J_g) \equiv \frac{1}{\Delta V_{ij}}\left[\Delta_i(\vec{\Omega}\vec{n}\Delta l r J_g) + \Delta_j(\vec{\Omega}\vec{n}\Delta l r J_g)\right] - \frac{\Delta S_{ij}}{\Delta V_{ij}}\frac{\Delta_k(\eta J_g)}{\Delta\phi_k},$$

$$(\vec{\Omega}\vec{n}\Delta l)_i = +\xi\Delta z_i - \mu\Delta r_i = +\xi(z_{i,j+1} - z_{ij}) - \mu(r_{ij+1} - r_{ij}),$$

$$(\vec{\Omega}\vec{n}\Delta l)_j = -\xi\Delta z_j + \mu\Delta r_j = -\xi(z_{i+1,j} - z_{ij}) + \mu(r_{i+1,j} - r_{ij}),$$

where indices (i, j) are cell indices; $k = 1,2,...,K_m$; $m = 1,2,...,M$.

To ensure closure, the system of equations of the DS_n-technique (1.4) is supplemented with the boundary conditions and relationships between the values, which J has at the center and sides of the cells. These relations are constructed in compliance with the flux direction at the sides.

The characteristic feature of radiation transport problems is that optic densities vary widely through space and time. High densities bring large problems for the method of discrete coordinates, causing non-monotonicity in the solution. This is the result of anti-dissipation terms in the remainder of the second order scheme (DD-scheme).

To improve monotonic properties of the DS_n-technique with respect to special variables, artificial dissipation is introduced:

$$\frac{1}{c\Delta t}\left[(J_g)^{n+1} - (J_g)^n\right] + div_h(\vec{\Omega}\Psi_g) + \alpha_g J_g = Q_g, \tag{1.5}$$

where dissipative function of distribution Ψ_g is in the following relation with function J_g

$$J_g = \Psi_g + \delta_g h div_h(\vec{\Omega}\Psi_g) - \theta_g h div_h\left(\vec{\Omega}\tilde{Q}_g\right), \tag{1.6}$$

where h is a linear size of a cell, δ_g, θ_g are dissipation coefficients, $\tilde{Q}_g = Q_g + \frac{1}{c\Delta t}(J_g)^n$.

Substituting the expression of Ψ for J in (1.5) yields a transport equation with artificial dissipation and additional summands with second derivatives.

$$\frac{1}{c\Delta t}\left[(J_g)^{n+1} - (J_g)^n\right] + div_h(\vec{\Omega}J_g) + \alpha_g J_g = Q_g + \delta_g h\, div_h(\vec{\Omega}J_g) - \theta_g h div_h\left(\vec{\Omega}\tilde{Q}_g\right) + o(h^2).$$

By selecting the coefficients δ_g, θ_g we try to suppress anti-dissipation resulted in the DD-scheme.

Substituting J from (1.6) in (1.5), obtain an equation of Ψ function:

$$\tilde{\alpha}_g\Psi_g + (1 + \delta_g h\tilde{\alpha}_g) div_h(\vec{\Omega}\Psi_g) = \tilde{\alpha}_g\left[\frac{\tilde{Q}_g}{\tilde{\alpha}_g} + \tilde{\alpha}_g\theta_g\Delta h div_h\left(\vec{\Omega}\frac{\tilde{Q}_g}{\tilde{\alpha}_g}\right)\right], \tag{1.7}$$

where $\tilde{\alpha}_g = \frac{1}{c\Delta t} + \alpha_g$. Assuming that parameter $\tilde{\alpha}_g$ is constant in the cell under consideration, it is introduced under the sign $div_h\left(\vec{\Omega}\tilde{Q}_g\right)$.

In the iteration solution of the transport equation, Q_g value in (1.7) is taken from previous outer iteration, i.e. Q_g^{ν}. Since the obtained system of equations is integral-differential, an iteration method is applied with respect to the right-hand side of the transport equation incorporating the collision integral and independent source in the form of the Planck function:

$$Q_g^\nu = \frac{1}{4\pi}\left(\alpha_{sg}^\nu U_g^\nu + \alpha_{cg}^\nu B_g\left(T^\nu\right)\right), \tag{1.8}$$

$$div_h(\vec{\Omega}Q_g^\nu) \equiv \frac{1}{\Delta V_{ij}}\left[\Delta_i(\vec{\Omega}\vec{n}\Delta lrQ_g^\nu) + \Delta_j(\vec{\Omega}\vec{n}\Delta lrQ_g^\nu)\right] - \frac{\Delta S_{ij}}{\Delta V_{ij}}\frac{\Delta_k(\eta Q_g^\nu)}{\Delta\phi_k}.$$

Here Q_g^ν values at the cell sides are determined as half-sums at the centers of the adjacent cells.

Introducing the reduced absorption coefficient $\alpha_g^* = \dfrac{\tilde{\alpha}_g}{1+\delta_g h\tilde{\alpha}_g}$, write down Eq. (1.7) as

$$\alpha_g^*\Psi_g + div_h(\vec{\Omega}\Psi_g) = \alpha_g^* Q_g^*, \tag{1.9}$$

где $Q_g^* = \dfrac{\tilde{Q}_g}{\tilde{\alpha}_g} + \tilde{\alpha}_g\theta_g h div_h\left(\vec{\Omega}\dfrac{\tilde{Q}_g}{\tilde{\alpha}_g}\right)$.

Parameters δ_g, θ_g are selected from the conditions of infinitesimal of $J_g - \Psi_g = O\left(\Delta x^2\right)$ and monotonic properties of the solution to Eq. (1.9) in optically thick medium. To solve Eq. (1.9), apply discrete coordinate method of the second order of accuracy (DD-scheme). Construction of the scheme itself and method for solving the difference equations based on the ordering are similar to those used in Ref. /9/.

The obtained scheme can be presented in the mesh-characteristic form:

$$\alpha_g^*\frac{\left(\Psi_g\right)_{s+1} + \left(\Psi_g\right)_s}{2} + \frac{\left(\Psi_g\right)_{s+1} - \left(\Psi_g\right)_s}{\Delta x_s} = \alpha_g^* Q_g^*, \tag{1.10}$$

$$div_h(\vec{\Omega}\Psi_g) = \frac{\left(\Psi_g\right)_{s+1} - \left(\Psi_g\right)_s}{\Delta x_s}.$$

Here Ψ_s – is a value of function Ψ at the point where the characteristic cuts the hyperplane passing through the centers of the lit sides; Ψ_{s+1} – is a value of function Ψ at the point where the characteristic cuts the hyperplane passing through the centers of the unlit sides; $\Delta x_s = x_{s+1} - x_s$ is a distance between these two points along the characteristic. Depending on the number of the lit and unlit sides, obtain formulas for $\Psi_s, \Psi_{s+1}, \Delta x_s$:

$$\Psi_s = \left[-\sum_l\left(\vec{\Omega}\vec{n}\Delta lr\Psi\right)_l + \frac{\Delta S_{ij}}{\Delta\phi_k}\eta_k\Psi_k\right]\left[-\sum_l\left(\vec{\Omega}\vec{n}\Delta lr\right)_l + \frac{\Delta S_{ij}}{\Delta\phi_k}\eta_k\right]^{-1},$$

l – index of a lit side;

$$\Psi_{s+1} = \left[\sum_{\text{€}}\left(\vec{\Omega}\vec{n}\Delta lr\Psi\right)_{\text{€}} + \frac{\Delta S_{ij}}{\Delta\phi_k}\eta_{k+1}\Psi_{k+1}\right]\left[\sum_{\text{€}}\left(\vec{\Omega}\vec{n}\Delta lr\right)_{\text{€}} + \frac{\Delta S_{ij}}{\Delta\phi_k}\eta_{k+1}\right]^{-1},$$

€ – index of a unlit side;

$$\Delta x_s = \Delta V_{ij}\left[\sum_{\text{€}}\left(\vec{\Omega}\vec{n}\Delta lr\right)_{\text{€}} + \frac{\Delta S_{ij}}{\Delta\phi_k}\eta_{k+1}\right]^{-1} = \Delta V_{ij}\left[-\sum_l\left(\vec{\Omega}\vec{n}\Delta lr\right)_l + \frac{\Delta S_{ij}}{\Delta\phi_k}\eta_k\right]^{-1}.$$

Now select parameters δ_g, θ_g so that solutions to Eqs. (1.10) coincide with the exact solution to the initial transport equation in the characteristic form within the interval $\left[x_s \le x \le x_{s+1}\right]$:

$$\frac{\partial J_g}{\partial x} + \tilde{\alpha}_g J_g = \tilde{Q}_g. \tag{1.12}$$

Assume $\tilde{\alpha}_g$ to be constant in the cell within the interval $[x_s, x_{s+1}]$ and $\tilde{Q}_g$ to be linear:

$$\widetilde{Q}_g(x)=\frac{\left(\widetilde{Q}_g\right)_s+\left(\widetilde{Q}_g\right)_{s+1}}{2}+\frac{x-x_{s+1/2}}{\Delta x_s}\left[\left(\widetilde{Q}_g\right)_{s+1}-\left(\widetilde{Q}_g\right)_s\right].$$

Then obtain

$$\left(J_g\right)_{s+1}=\exp\left(-\widetilde{\alpha}_g\Delta x_s\right)\left(J_g\right)_s+\left(1-\exp\left(-\widetilde{\alpha}_g\Delta x_s\right)\right)\frac{\left(\widetilde{Q}_g\right)_{s+1}-\left(\widetilde{Q}_g\right)_s}{-\widetilde{\alpha}_g{}^2\Delta x_s}+\frac{1}{\widetilde{\alpha}_g}\left(\left(\widetilde{Q}_g\right)_{s+1}-\left(\widetilde{Q}_g\right)_s\exp\left(-\widetilde{\alpha}_g\Delta x_s\right)\right).$$

Then assuming equality of the values at the lit sides $\left(\Psi_g\right)_s=\left(J_g\right)_s$, require output values to be the same $\left(\Psi_g\right)_{s+1}=\left(J_g\right)_{s+1}$. Selecting δ_g parameter from this value, obtain

$$\delta_g=\frac{1}{2}\frac{1+\exp\left(-\widetilde{\alpha}_g\Delta x_s\right)}{1-\exp\left(-\widetilde{\alpha}_g\Delta x_s\right)}-\frac{1}{\widetilde{\alpha}_g\Delta x_s},\ \ \theta_g=\frac{1}{\widetilde{\alpha}_g}\delta_g,\ h=\Delta x_s. \tag{1.13}$$

Then difference $J_g-\Psi_g$ becomes as follows

$$J_g-\Psi_g=-\frac{\delta_g\Delta x}{\alpha_g^*}div_h\left(\vec{\Omega}div_h\left(\vec{\Omega}\Psi_g\right)\right)+\left(\delta_g\Delta x\right)^2div_h\vec{\Omega}\left(div_h\vec{\Omega}\frac{\widetilde{Q}_g}{\widetilde{\alpha}_g}\right). \tag{1.14}$$

Now estimate value of $J_g-\Psi_g$ taking into account that $0\le\delta_g\le 0.5,\quad 0\le\alpha_g^*\Delta x\le 2$. At $\widetilde{\alpha}_g\Delta x<1$ taking a Taylor series expansion of $\exp\left(-\widetilde{\alpha}_g\Delta x\right)$, derive the following estimate $\frac{\delta_g\Delta x}{\alpha_g^*}=\frac{\delta_g\Delta x}{\widetilde{\alpha}_g}\left(1+\delta_g\Delta x\widetilde{\alpha}_g\right)=\frac{\Delta x^2}{12}+O\left(\Delta x^3\right)$. And if $\widetilde{\alpha}_g\Delta x\ge 1$, then $\frac{\delta_g\Delta x}{\alpha_g^*}=\frac{\delta_g\Delta x}{\widetilde{\alpha}_g}+\left(\delta_g\Delta x\right)^2\le 2\delta_g\Delta x^2<\Delta x^2$. Based on this, obtain the following estimate $J_g-\Psi_g=O\left(\Delta x^2\right)$.

So we have the following. Instead of solving Eq. (1.4), where optical thickness $\widetilde{\alpha}_g\Delta x$ might be large and application of the DD-scheme would lead to significant approximation-induced oscillations, we solve Eqs. (1.9) with respect to dissipative function Ψ_g. In this new problem, optical thickness is small $\alpha_g^*\Delta x<2$ and application of the DD-scheme would not lead to the oscillations mentioned above. At the same time solution of the new problem is close to solution of the initial one: $J_g-\Psi_g=O\left(\Delta x^2\right)$.

Using the selected parameters (1.13), start solving transport equation (1.7) with the DD-scheme. Computation is done according to the recurrent scheme with the ordering procedure /10/. If in some cell $\Psi_g<0$ for some direction, this means that in this cell we transit to the first-order scheme ($\delta_g=0.5,\ \theta_g=0.5$), i.e. computation is done according to the DD/St-scheme.

After values of Ψ_g are determined, obtain radiation intensity at the cell center:

$$\left(J_g^{\nu+1/2}\right)_{i+\frac{1}{2},j+\frac{1}{2},k-\frac{1}{2},m-\frac{1}{2}}=\frac{1}{\widetilde{\alpha}_g\Delta V_{ij}}\left\{(Q_g^\nu+\frac{J_g^n}{c\Delta t})\Delta V_{ij}-\left[\Delta_i(\vec{\Omega}\vec{n}\Delta lr\Psi_g^{\nu+1/2})+\Delta_j(\vec{\Omega}\vec{n}\Delta lr\Psi_g^{\nu+1/2})\right]-\right.$$
$$\left.-\Delta S_{ij}\frac{\Delta_k(\eta\Psi_g^{\nu+1/2})}{\Delta\phi_k}\right\}. \tag{1.15}$$

Then the next cell is computed and so on until all cells are processed in this specific direction $\vec{\Omega}_{k-1/2,m-1/2}$. Then a loop over directions $\vec{\Omega}$ is done till al directions are treated for a specific group. After that we start treating next group g till all groups are considered. When this work is finished, the second stage (acceleration) is started.

As a rule, simple source iterations converge slowly, especially in presence of optically dense layers. So, acceleration of the iteration convergence is a very important factor in improving efficiency of simulations solving the equations of radiation transport.

To accelerate the iteration convergence, the diagonal matrix technique (DMT) is implemented in the DDAD technique. This approach was earlier used in [5] and [6]. It is easier than the diffusion-synthetic method (DSA-method [7]) but helps significantly accelerate simple iterations though conceding the DSA method on the convergence rate. The DMT was adapted to the DDAD-scheme on arbitrary quadrilateral meshes [1]. If, similarly to Jacoby-type iterations, radiation density at some point in the system of radiation transport equations is expressed via the Planck function at the same point, and then substituted in the energy equation, the obtained system of equations will give a diagonal matrix with respect to temperature. Using the obtained temperature, it is possible to solve the initial system either by running 1D case or with iteration methods in 2D case. This approach in 1D plane case was proposed in Ref. /11/ for the first-order scheme. In the presented technique this approach is applied to the second-order DDAD-scheme in 2D case.

Consider the energy equation, which is being solved jointly with the radiation transport equation:

$$\rho \frac{E^{n+1} - E^n}{\Delta t^n} = \sum_{g=1}^{G} \alpha_{cg} (U_g^{n+1} - B_g^{n+1}) + \rho Q,$$

where $B_g^{n+1} = B_g\left(T^{n+1}\right)$.

Energy equation for the $\nu+1$-th iteration:

$$\rho(E^{\nu+1} - E^n) = \Delta t^n \sum_{g=1}^{G} \alpha_{cg} (U_g^{\nu+1} - B_g^{\nu+1}) + \Delta t^n \rho Q.$$

Linearize the internal energy and the Planck function with respect to temperature:

$$\left[E^{n+1}(T)\right]^{k+1} = \left[E^{n+1}(T)\right]^k + E_T^k\left(T^{k+1} - T^k\right),$$

$$\left[B_g^{n+1}(T)\right]^{k+1} = \left[B_g^{n+1}(T)\right]^k + B_{gT}^k\left(T^{k+1} - T^k\right),$$

where $E_T^k = \left(\frac{\partial E}{\partial T}\right)^k, B_{gT}^k = \left(\frac{\partial B_g}{\partial T}\right)^k$.

From the transport system derive $U_g^{\nu+1}$:

$$U_g^{\nu+1} = U_g^{\nu+1/2} + \Delta U_g^{\nu+1} = U_g^{\nu+1/2} + b_g(B_g^{\nu+1} - B_g^{\nu}), \tag{1.16}$$

where $b_g = \dfrac{\alpha_{cg}}{\dfrac{1}{c\Delta t} + \alpha_{cg} + d_g^{\nu+1/2}}$,

$$d_g^{\nu+1/2} = \frac{\dfrac{1}{\Delta V_{ij}} \sum_{m=1}^{M} \sum_{k=1}^{K_m} (a\Psi_g^{\nu+1/2})_{k-1/2,m-1/2} \Delta\mu_{m-1} \Delta\phi_{k-1}}{U_g^{\nu+1/2}}.$$

Substituting $U_g^{\nu+1}$ in the energy equation linearized with respect to temperature, obtain:

$$T^{k+1} = T^k + \left\{\rho(E^n - E^k) + \Delta t^n \rho Q + \Delta t^n \sum_{g=1}^{G}\left[\alpha_{cg}\left(U_g^{\nu+1/2} + b_g(B_g(T^k) - B_g^{\nu})\right) - \alpha_{cg} B_g(T^k)\right]\right\} \times$$

$$\times \left\{\rho E_T^k + \Delta t \sum_{g=1}^{G}\left[\alpha_{cg}(1 - b_g)\right] B_{gT}^k\right\}^{-1}.$$

When Newton iterations k converge, obtain temperature $T^{\nu+1} = T^{k+1}$. Using the new temperature obtain $B_g^{\nu+1}$ at the cell center and density $U_g^{\nu+1}$ according to formula (1.16). Outer iterations ν are done when $U_g^{\nu+1}$ and $T^{\nu+1}$ converge.

2. Numerical calculations of the test problems

Test 1. Solution of the system of non-stationary radiation transport equations accounting for radiation spectrum and ignoring scattering due to non-homogeneous medium (the Fleck problem).

Planck radiation flux corresponding to the material temperature of T=1 hits the surface of a 4cm-thick flat layer. The layer consists of three physical regions. Since the DDAD technique is good for axi-symmetrical geometry, the flat layer in each problem under consideration is replaced with a spherical one located at the distance of 100 cm from the axis of symmetry (Fig.1).

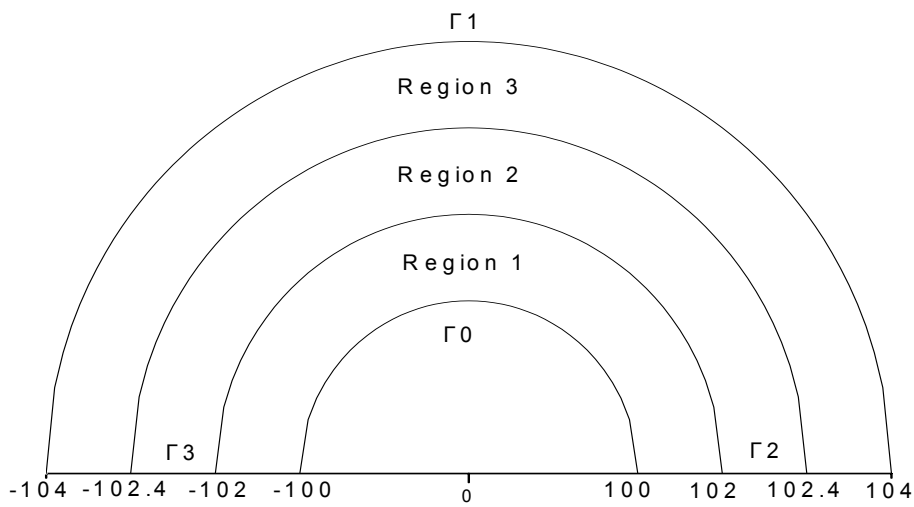

Fig.1 Problem geometry.

This problem is interesting since the standard iteration method gives very slow convergence, therefore, acceleration is needed.

Spectral boundary conditions at the upper boundary Γ1 were as follows: $J_g = 0$ at $\vec{\Omega} \cdot \vec{n} < 0$ (free surface). At the lower boundary Γ0 they were: $J_g = \frac{1}{4\pi} B_g(T=1)$ at $\vec{\Omega} \cdot \vec{n} < 0$. Boundary conditions at the axis of symmetry Z (boundaries Γ2 and Γ3) were implemented by exploiting symmetry $J_g(t,0,z,\mu,\psi) = J_g(t,0,z,\mu,\pi-\psi), \quad \psi < \frac{\pi}{2}$.

The absorption coefficient was calculated by formula $\alpha_c = \frac{\chi(1-e^{-\varepsilon/T})}{\varepsilon^3}$, χ = 27 in regions 1 and 3, and χ = 10000 in region 2. The scattering coefficient was - $\alpha_s = 0$.

Initial temperature in regions 1, 2 and 3 was $T_{1,2,3}$ = 0.001, the equation of state was $E_{1,2,3}$ = 0.81T, and material density was $\rho_{1,2,3}$=1.

For energy variable the calculations used the following mesh: ε_g =15.0, 12.0, 10.0, 8.0, 7.0, 6.0, 5.5, 5.0, 4.5, 4.0, 3.5, 3.0, 2.6, 2.2, 1.8, 1.4, 1.0, 0.7, 0.5, 0.4, 0.3, 0.2, 0.15, 0.1, 0.08, 0.06, 0.04, 0.02, 0.0 (28 groups).

The mesh in the direction space $\vec{\Omega}$ corresponds to the ES_{12} quadrature.

In terms of space intervals in radial direction, the mesh was non-uniform in each region and used the formula: $100+r_1$, where r_1= 0, 0.004, 0.04, r_4 = 0.1, . . . , r_{22} = 1.9 (18 uniform intervals with Δr = 0.1), r_{23} = 1.987, 1.999, 2, 2.001, 2.004, 2.013, r_{29} = 2.04, . . . , r_{37} = 2.36 (8 uniform intervals with Δr = 0.04), r_{38} = 2.396, 2.4, 2.404, 2.44, r_{42} = 2.5, . . . , r_{57} = 4 (15 uniform intervals with Δr = 0.1) ($\hat{i}$ = 57). Number of intervals in regions 1, 2, and 3 was 24, 14, and 18, respectively. In terms of angular spacing, the mesh was uniform with 40 intervals in each region.

Time step was τ = 0.0002. At each time step the solution was iteratively calculated till accuracy of 0.1% (ε_{cx}=0.001) was reached for the calculated material temperature. Calculations were done according to the first- and second-order approximation. First-order St-scheme was calculated with parameters $\delta = 0.5, \quad \theta = 0.5$. The classic DD/St-scheme leads to divergence of iterations.

Though the unity temperature follows from the boundary conditions, numerical calculations did not give it. The reason is that the boundary conditions are specified for the intensity, and temperature at the boundary was calculated from the energy equation. Temperature at the boundary was less than a unity and approached it when radiation-emitting region heated up.

The calculation results are given in the plots showing material temperature versus spatial variable. Figure 2 presents profiles of material temperature obtained with the first-order (St-scheme) and second-order (DDAD-scheme) schemes on the coarse (56 intervals in radius) mesh at computational time ct=9 cm. The results are compared with the exact solution obtained on the fine mesh (4000 points in radial direction).

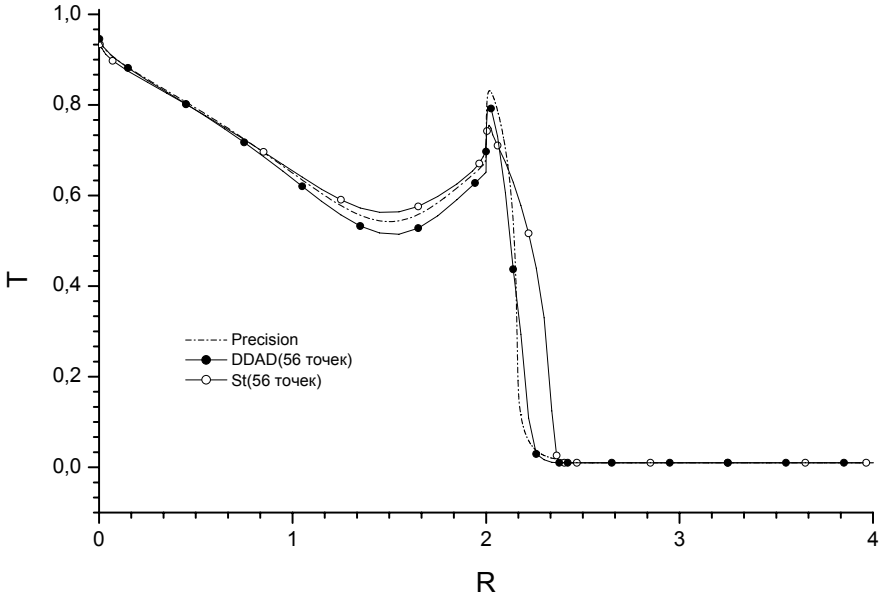

Fig. 2 Profile of the material temperature at ct =9 cm.

Figure 2 shows that the first-order scheme, unlike the second-order one, smears the front of the heat wave traveling through the optically thick medium (the 2nd region).

Figure 3 shows profiles of the material temperature obtained with the first-order (St-scheme) and second-order (DDAD-scheme) schemes on a fine (168 intervals in radial direction) mesh and a coarse (56 intervals in radial direction) one at the computational time ct=400 cm. At ct=400 cm the solution becomes stationary and is compared to the exact solution obtained at 4000 points on the radius.

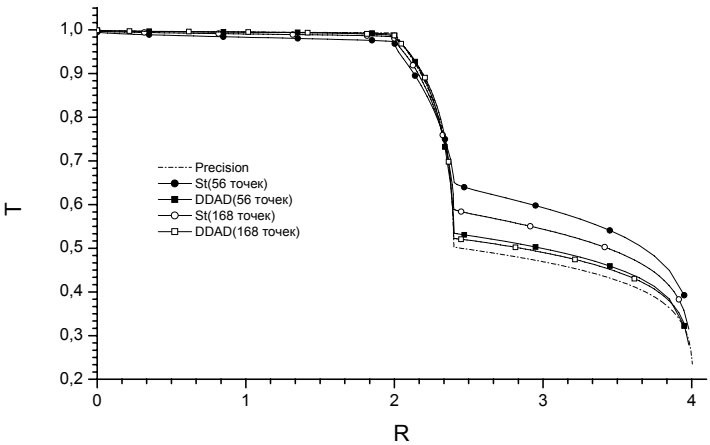

Fig.3 Profile of the material temperature at ct=400.

From Fig.3 it is obvious that DDAD-scheme of the second order gives a monotonic profile close to the exact solution. If compared with the first-order St-scheme, DDAD-scheme with mesh refining gives a faster convergence to the exact solution.

Test 2. The exact solution of a system of non-stationary spectral radiation transport equations with no account for scattering in the homogeneous medium

Radiation of intensity $J_g = \dfrac{2\varepsilon_g{}^3}{(0.04 - 0.037(\vec{\Omega}\vec{n}))[e^{\frac{\nu}{T}} - 1]}$, or T=$5(t - 0.0466x_0)$, is incident on a plane layer 4 cm thick. The layer contains one physical region. The initial temperature in the region is T=0.01, the equation of state is E=152.73T^4; material density is ρ=1. The absorption factor was calculated as $\alpha_g = \dfrac{\varepsilon_g e^{\varepsilon_g/T}}{4T^2(e^{\varepsilon_g/T} - 1)}$. The scattering factor was $\alpha_s = 0$.

To obtain a 2D axially symmetric configuration, the planar layer is replaced by a spherical one 100 cm distant from the symmetry axis (Fig.1).

Boundary conditions

Γ1: $J_g = 0$ for $\vec{\Omega} \cdot \vec{n} < 0$ (free surface)

$$\Gamma 0: J_g(x_0 = 100, t, (\vec{\Omega}\vec{n}) < 0) = \frac{2\varepsilon_g^3}{[0.04 - 0.037(\vec{\Omega}\vec{n})][e^{\frac{\varepsilon_g}{5(t-0.0466x_0)}} - 1]}, \quad x = \sqrt{r^2 + z^2}$$

Γ2, Γ3 (the symmetry axis Z): $J_g(t,0,z,\mu,\psi) = J_g(t,0,z,\mu,\pi - \psi), \quad \psi < \dfrac{\pi}{2}$

Initial conditions

t_0=4.66, $J_g(t_0, r, z, \mu, \psi) = 0$

Energy intervals: ε_g =15.0, 12.0, 10.0, 8.0, 7.0, 6.0, 5.5, 5.0, 4.5, 4.0, 3.5, 3.0, 2.6, 2.2, 1.8, 1.4, 1.0, 0.7, 0.5, 0.4, 0.3, 0.2, 0.15, 0.1, 0.08, 0.06, 0.04, 0.02, 0.0 (28 groups)

The mesh in the direction space $\vec{\Omega}$ corresponds to the ES_{12} quadrature.

Radial spacing: 40 intervals of equal length (Δr = 0.1)

Angular spacing: 40 intervals of equal length

Constant time step $\Delta t = 2 \cdot 10^{-4}$

Temperature iteration convergence constant ε_{cx} =0.0001

The numerical solution was compared with the analog of the exact solution /2,3/ obtained for the 1D plane case:

$$T = \begin{cases} 5(t - 0.0466x), & t > 0.0466x, \quad x = \sqrt{r^2 + z^2}, \\ 0, & t \le 0.0466x, \end{cases}$$

$$J_\nu = \begin{cases} \dfrac{200\nu^3}{(4 - 3.7(\vec{\Omega}\vec{n}))\{\exp[\nu / T] - 1\}}, & t > 0.0466x, \\ 0\ , & t \le 0.0466x. \end{cases}$$

The calculation was run until the heat wave reached the right boundary, i.e., to t = 4.85.

Figure 4 shows temperatures obtained with the first-order St-scheme and the second-order DDAD-scheme for times t = 4.7, 4.75, 4.8, 4.85.

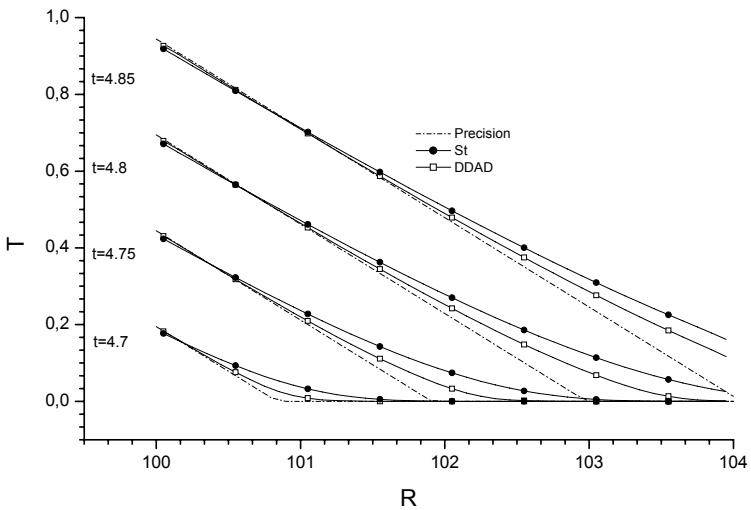

Fig. 4. Temperatures at times t = 4.7, 4.75, 4.8, 4.85

It is obvious, that the obtained solutions are in a good agreement with the exact solution.

Test 3: The exact solution of a system of non-steady 'gray' radiation transport equations with no account for scattering in the two-material region

"Gray" radiation of intensity $J = \dfrac{29(307 + 1000t)}{90 + 87(\vec{\Omega}\vec{n})}$, or $T = 0.195\sqrt[4]{1000t + 307}$, is incident on a flat layer that is 5 cm thick and consists of two materials of unit density.

Equation of state: $E = \begin{cases} 1.242T^4, x \in [101,103], \\ 10.047T^4, x \in [103,106]. \end{cases}$

Scattering factor: $\alpha_s = 0$.

The absorption factor is calculated as

$$\alpha_c = \begin{cases} \left(981.18T^4\right)^{-1}, x \in [101,103], \\ \left(327.06T^4\right)^{-1}, x \in [103,106]. \end{cases}$$

To obtain a 2D axially symmetric configuration, the planar layer is replaced by a spherical one 100 cm distant from the symmetry axis (Fig.1).

<u>Boundary conditions</u>

$\Gamma 1$: $J(x_1 = 106, t, (\vec{\Omega}\vec{n}) < 0) = \dfrac{29(318 + 1000t)}{90 + 87(\vec{\Omega}\vec{n})}, \quad x = \sqrt{r^2 + z^2}$

Γ0: $J(x_0 = 100, t, (\vec{\Omega}\vec{n}) < 0) = \dfrac{29(307 + 1000t)}{90 + 87(\vec{\Omega}\vec{n})}, \quad x = \sqrt{r^2 + z^2}$

Γ2, Γ3 (symmetry axis Z): $J(t,0,z,\mu,\psi) = J(t,0,z,\mu,\pi - \psi), \quad \psi < \dfrac{\pi}{2}$.

<u>Initial conditions</u>

For t_0=0, a continuous function J_g and a piecewise continuous function T are defined:

$$J(t_0, r, z, \mu, \psi) = \begin{cases} \dfrac{29(x + 206)}{90 + 87(\vec{\Omega}\vec{n})}, & x \in [101,103], \quad x = \sqrt{r^2 + z^2}, \\ \dfrac{87x}{90 + 87(\vec{\Omega}\vec{n})}, & x \in [103,106], \end{cases}$$

and piecewise-continuous function T:

$$T(t_0, r, z) = \begin{cases} 0.195\sqrt[4]{x + 206}, & x \in [101,103), \quad x = \sqrt{r^2 + z^2}, \\ 0.24\sqrt[4]{x}, & x \in (103,106]. \end{cases}$$

The mesh in the direction space $\vec{\Omega}$ corresponds to the ES_{12} quadrature.

Radial spacing: 40 intervals of equal length in region 1 (Δr=0.05) and 40 intervals of equal length in region 2 (Δr=0.075))

Angular spacing: 40 intervals of equal length

Constant time step $\Delta t = 2*10^{-4}$

Temperature iteration convergence constant ε_{cx}=0.0001

The numerical solution was compared with the analog of the exact solution /4,5/ obtained for the 1D plane case:

$$J(t, r, z, \mu, \psi) = \begin{cases} \dfrac{29(x + 1000t + 206)}{90 + 87(\vec{\Omega}\vec{n})}, & x \in [101,103], \quad x = \sqrt{r^2 + z^2}, \\ \dfrac{29(3x + 1000t)}{90 + 87(\vec{\Omega}\vec{n})}, & x \in [103,106], \end{cases}$$

$$T(t, r, z) = \begin{cases} 0.195\sqrt[4]{x + 1000t + 206}, & x \in [101,103), \quad x = \sqrt{r^2 + z^2}, \\ 0.182\sqrt[4]{3x + 1000t}, & x \in (103,106]. \end{cases}$$

Figure 5 shows temperatures obtained with the DDAD-scheme on fine (40+40) and coarse (5+5) meshes for t = 0.005, 0.01.

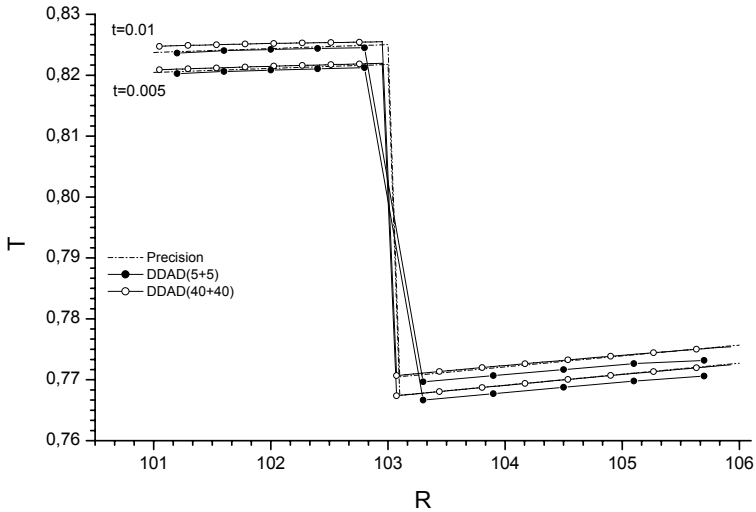

Fig. 5. Temperatures at t = 0.005, 0.01

It is obvious from Fig.5 that the solution obtained on the fine mesh agrees rather well with the exact solution.

Conclusion

As shown by calculations, the DDAD scheme in combination with the DMT-method of iteration acceleration performs rather effectively in the simulation of thermal radiation transport with the multi-group kinetic model on arbitrary quadrilateral meshes.

References

1. Fleck J.A., Cummings J.D. J. Comput. Phys., 1971, v.8, h.313-342
2. RFNC-VNIITF Report 10 under Contract B336978, 1997.
3. Andreyev, E.S., Dumkina, G.V., and Kozmanov M.Y., Certain exact solutions to a system of energy and non-steady spectral radiation transport equations. J. Computational Mathematics and Mathematical Physics, 1981, V.21, Is.4, p.1054-1055.
4. RFNC-VNIITF Report 11 under Contract B336978, 1997.
5. Andreyev, E.S., Kozmanov M.Y., and Rachilov, E.B., Exact solutions to radiation transport equations with interface discontinuity. J. Computational Mathematics and Mathematical Physics, 1984, V.24, Is.1, p.161-163.
6. Karlson B., Numerical solution of a neutron kinetics problem. In *Theory of Nuclear Reactors*, Moscow, ATOMIZDAT Publishers, 1963, p.243-258.
7. Reed W.H. New difference schemes for the neutron transport equation. Nucl.Sci.Eng., Vol.46, No.2, pp.309-314,1971.
8. Kozmanov, M.Y., VANT, Is.2, 1989, p.51-54.
9. Troschiev, V.E., and Shumilin, V.A., A finite-difference scheme to solve the 2D transport equation on irregular quadrangular meshes. J. Computational Mathematics and Mathematical Physics, 1986, V.26, Is.2, p.230-241.
10. Troschiev, V.E., Mesh classes permitting conservative approximations of the 2D transport operator by the triangular difference operator. J. Computational Mathematics and Mathematical Physics, 1976, V.16, Is.3, p.793-797.
11. Gusev, V.Y., Kozmanov, M.Y., and Rachilov, E.B., A method of solving implicit finite-difference equations approximating radiation transport and diffusion equations. J. Computational Mathematics and Mathematical Physics, 1984, V.24, Is.12, p.1842-1849.